Determining the shear viscosity of model liquids from molecular dynamics simulations

Hess, Berk

Published in:
Journal of Chemical Physics

DOI:
10.1063/1.1421362

Publication date:
2002

Determining the shear viscosity of model liquids from molecular dynamics simulations

Berk Hess

Citation: J. Chem. Phys. **116**, 209 (2002); doi: 10.1063/1.1421362
View online: https://doi.org/10.1063/1.1421362
View Table of Contents: http://aip.scitation.org/toc/jcp/116/1
Published by the American Institute of Physics

Determining the shear viscosity of model liquids from molecular dynamics simulations

Berk Hess[a)]
Department of Biophysical Chemistry, University of Groningen, Nijenborgh 4, 9747 AG Groningen, The Netherlands

(Received 8 June 2001; accepted 2 October 2001)

Several methods are available for calculating shear viscosities of liquids from molecular dynamics simulations. There are equilibrium methods based on pressure or momentum fluctuations and several nonequilibrium methods. For the nonequilibrium method using a periodic shear flow, all relevant quantities, including the accuracy, can be estimated before performing the simulation. We compared the applicability, accuracy and efficiency of this method with two equilibrium methods and another nonequilibrium method, using simulations of a Lennard-Jones fluid and the SPC and SPC/E [(extended) simple point charge] water models. © *2002 American Institute of Physics.* [DOI: [10.1063/1.1421362]

I. INTRODUCTION

The shear viscosity is a property of liquids which can be determined easily by experiment. It is useful for parametrizing the force field, because it is a kinetic property, while most other properties which are used for parametrization are of a thermodynamic nature. It is not only important for pure liquids, as it also influences the rates of (rotational) diffusion and conformational change of molecules solvated in the liquid.

Several methods for determining the shear viscosity are described in the literature. From an equilibrium simulation the viscosity can be obtained from pressure or momentum fluctuations.[1] There are two nonequilibrium methods that make use of steady-state shear. One can use a periodic shear flow,[2] or use sliding boundary conditions, for instance the commonly used SLLOD[3] algorithm.[4] All the methods mentioned above, except for the momentum fluctuation approach, are described in Allen and Tildesley.[5] A recent method uses momentum pulse relaxation.[6] The authors claim that, unlike the periodic shear flow method, their method is not wavelength or box-size dependent since acoustic modes cannot travel across the box boundaries. However, acoustic modes are not the origin of the wavelength dependence. Steady shear does not induce density fluctuations in a liquid and thus also no acoustic waves. The momentum pulse relaxation method suffers from the same wavelength dependence as the periodic shear flow method, since in both methods the size of the perturbation is of the order of the simulation box.

We will describe the two equilibrium methods, the periodic shear flow method and the SLLOD algorithm in more detail. We will show applications of these four methods to a Lennard-Jones fluid and two water models.

a)Electronic mail: hess@chem.rug.nl

II. PRESSURE FLUCTUATIONS

The shear viscosity of a liquid is related to the fluctuations of the off-diagonal elements of the pressure or stress tensor. The viscosity can be calculated from an equilibrium simulation by integrating the Green–Kubo formula:[7]

$$\eta = \frac{V}{k_B T} \int_0^\infty \langle P_{xz}(t_0) P_{xz}(t_0+t) \rangle_{t_0} \mathrm{d}t. \tag{1}$$

This can be reformulated as an Einstein relation:

$$\eta = \lim_{t\to\infty} \frac{1}{2} \frac{V}{k_B T} \frac{\mathrm{d}}{\mathrm{d}t} \left\langle \left(\int_{t_0}^{t_0+t} P_{xz}(t') \mathrm{d}t' \right)^2 \right\rangle_{t_0}. \tag{2}$$

Both methods converge very slowly, because the pressure in a volume of the size of a simulation box fluctuates heavily. The asymptotic behavior of the pressure autocorrelation is $t^{-3/2}$, which makes an accurate estimation of the viscosity difficult. The Einstein relation is more convenient to use, since the inaccuracies in the long time correlations can be ignored by only considering integrals over shorter times.

III. MOMENTUM FLUCTUATIONS

The viscosity can also be determined from transverse-current correlation functions for plane waves. The behavior of the velocity $\mathbf{u}(\mathbf{r},t)$ of a liquid is described by the Navier–Stokes equation:

$$\rho \frac{\partial \mathbf{u}}{\partial t} + \rho(\mathbf{u}\cdot\boldsymbol{\nabla})\mathbf{u} = \rho\,\mathbf{a} - \nabla p + \eta\,\nabla^2 \mathbf{u}, \tag{3}$$

where $\mathbf{a}$ is the external force per unit of mass and volume. Consider an incompressible liquid with an initial velocity field consisting of a plane wave in one direction:

$$\mathbf{u}(\mathbf{r},0) = \begin{pmatrix} u_0 \cos(k z) \\ 0 \\ 0 \end{pmatrix}. \tag{4}$$

The y and z-component of $\mathbf{u}$ will remain zero; for the x-component the Navier–Stokes equation reduces to

$$\frac{\partial u_x(z,t)}{\partial t} = \frac{\eta}{\rho} \frac{\partial^2 u_x(z,t)}{\partial z^2}. \tag{5}$$

The solution is

$$u_x(z,t) = u_0 \, e^{-t/\tau_r} \cos(k z), \tag{6}$$

$$\tau_r = \frac{\rho}{\eta k^2}. \tag{7}$$

From the solution it can be seen that plane waves decay exponentially with a time constant which is inversely proportional to the viscosity and proportional to the wavelength squared. According to the fluctuation–dissipation theorem the response of the system to internal fluctuations is the same as to a small external perturbation, such as initial condition (4). This means the viscosity can be determined from the autocorrelation of the amplitude of plane waves in the simulation box, which is also called the transverse-current correlation function. However, at short times the correlation function is not a pure exponential. To account for this, a phenomenological correction can be applied by incorporating a relaxation-time.[8,9] This changes Eq. (5) to

$$\frac{\partial u_x(z,t)}{\partial t} = \frac{\eta}{\rho} \int_0^t \phi(t-s) \frac{\partial^2 u_x(z,s)}{\partial z^2} \mathrm{d}s. \tag{8}$$

The most simple model for the memory kernel ϕ is

$$\phi(t) = \frac{1}{\tau_m} e^{-t/\tau_m}. \tag{9}$$

The solution of this equation with initial condition (4) is

$$u_x(z,t) = u_0 \, e^{-\beta} \left(\cosh(\Omega \beta) + \frac{1}{\Omega} \sinh(\Omega \beta) \right) \cos(k z), \tag{10}$$

where

$$\beta = \frac{t}{2\tau_m} \tag{11}$$

and

$$\Omega = \sqrt{1 - 4\tau_m \frac{\eta}{\rho} k^2}. \tag{12}$$

Note that although Ω can become imaginary, the solution will always be real. For large k the solution converges to the solution of the Navier–Stokes equation (6). The viscosity can be calculated by fitting the transverse-current correlation functions for different $\mathbf{k}$-vectors to formula (10).

Unfortunately the shear viscosity which is obtained using this method is dependent on $k = \|\mathbf{k}\|$. To obtain the macroscopic viscosity, one needs to extrapolate to $k = 0$. Palmer argues that since the viscosity in one dimension should be a symmetric function of k, one can approximate the viscosity in third order by

$$\eta(k) = \eta(0)(1 - ak^2) + O(k^4). \tag{13}$$

IV. THE PERIODIC PERTURBATION METHOD

Instead of measuring intrinsic fluctuations of the system, which have a fixed magnitude, we can apply an external force. The magnitude of this force can be chosen such that the effects are much easier to measure than the internal fluctuations. The external force will cause a velocity field $\mathbf{u}$ in the liquid according to the Navier–Stokes equation (3). We can choose the external force $\mathbf{a}$ such that a_y and a_z are zero and a_x is a function of z only. This makes u_y and u_z equal to zero. Since there is no pressure gradient in the x-direction, the equation for u_x becomes

$$\rho \frac{\partial u_x(z)}{\partial t} = \rho a_x(z) + \eta \frac{\partial^2 u_x(z)}{\partial z^2}. \tag{14}$$

The steady-state solution is given by

$$a_x(z) + \frac{\eta}{\rho} \frac{\partial^2 u_x(z)}{\partial z^2} = 0. \tag{15}$$

Since we will be using a periodic system in the simulations, the acceleration and velocity profile should also be periodic. To obtain a smooth velocity profile with small local shear rates, the acceleration profile should be smooth as well. A simple function which satisfies both conditions is a cosine:

$$a_x(z) = \mathcal{A} \cos(k z), \tag{16}$$

$$k = \frac{2\pi}{l_z}, \tag{17}$$

where l_z is the height of the box. When we take $u_z(x) = 0$ at $t = 0$, the generated velocity profile is

$$u_x(z) = \mathcal{V}(1 - e^{-t/\tau_r}) \cos(k z), \tag{18}$$

$$\mathcal{V} = \mathcal{A} \frac{\rho}{\eta k^2}, \tag{19}$$

where τ_r is given by (7). The Navier–Stokes equation is not valid for microscopic length-scales, therefore the wavelength should be at least an order of magnitude larger than the size of a molecule.

In an MD-simulation an acceleration can be added to each particle each MD step, according to Eq. (16). The average $\mathcal{V}$ can be measured and the viscosity can be calculated using the following formula:

$$\eta = \frac{\mathcal{A}}{\mathcal{V}} \frac{\rho}{k^2}. \tag{20}$$

We define the instantaneous $\mathcal{V}(t)$ in the simulation as follows:

$$\mathcal{V}(t) = 2 \sum_{i=1}^{N} m_i v_{i,x}(t) \cos(k \, r_{i,z}(t)) \Big/ \sum_{i=1}^{N} m_i, \tag{21}$$

where $v_{i,x}$ is the x-component of the velocity, $r_{i,z}$ is the z-coordinate and m_i is the mass of atom i. The average for $\mathcal{V}$ can be measured after the amplitude of the velocity profile has been fully developed, which is around $t = 5\tau_r$. To obtain the correct value for the viscosity the generated velocity profile should not be coupled to the heat bath, also the velocity profile should be excluded from the kinetic energy. One

would like $\mathcal{V}$ to be as large as possible to get good statistics. However, the shear rate should not be so high that the system moves too far from equilibrium. The maximum shear rate occurs where the cosine is zero, the rate is:

$$s_{\max} = \max_z \left| \frac{\partial v_x(z)}{\partial z} \right| = \mathcal{A} \frac{\rho}{\eta k}. \tag{22}$$

The system will be able to relax when the inverse shear rate is longer than the relaxation time. For most liquids this will be the rotation correlation time, which is around 10 picoseconds. When the shear rate is too high the apparent viscosity will be too low.

The accuracy of the viscosity estimate is determined by the momentum fluctuations described in the previous section. The amplitude of the fluctuation on $\mathcal{V}(t)$ is

$$\langle (\mathcal{V}(t) - \langle \mathcal{V}(t) \rangle)^2 \rangle^{1/2} = \sqrt{\frac{2 k_B T}{\rho V}}. \tag{23}$$

The 2 arises from the integral over $(2\cos)^2$ in (21); ρV is the total mass of the system. For large wavelengths the fluctuations have exponential correlation (10), with correlation time τ_r (7). From this the error in the average can be calculated. The relative standard error in the amplitude of the velocity profile is

$$\frac{\sigma_{\mathcal{V}}}{\mathcal{V}} = \sqrt{\frac{2\tau_r}{t_a}} \sqrt{\frac{2 k_B T}{\rho V}} \frac{s_{\max}}{k} = \frac{2}{s_{\max}} \sqrt{\frac{k_B T}{t_a \eta V}}, \tag{24}$$

where t_a is the time over which the average of $\mathcal{V}(t)$ is determined. The error in the viscosity is

$$\sigma_\eta = \frac{\sigma_{\mathcal{V}}}{\mathcal{V}} \eta = \frac{2}{s_{\max}} \sqrt{\frac{k_B T \eta}{t_a V}}. \tag{25}$$

The accuracy increases with the square root of time and the number of particles. When the CPU-time increases linearly with the number of particles, the CPU-time required for a given accuracy is independent of the system size. Thus a large system is optimal, since it produces a longer wavelength. The system should not be chosen too large, because the equilibration and shear development time increase as well.

The heat generated by the viscous friction is removed by coupling to a heat bath. Because this coupling is not instantaneous the real temperature of the liquid will be slightly lower than the observed temperature. Berendsen derived this temperature shift for coupling with the Berendsen thermostat.[10,11] We rewrote the shift in terms of the shear rate:

$$T_s = \frac{\eta \tau_c}{2 \rho C_v} s_{\max}^2, \tag{26}$$

where τ_c is the coupling time for the Berendsen thermostat and C_v is the heat capacity.

To get an idea of the order of magnitude of the quantities involved, we can look at a small simulation system for water at 20 °C:

$$\begin{aligned}
&\eta = 10^{-3}\ \mathrm{kg\,m^{-1}\,s^{-1}} && k = 1\ \mathrm{nm^{-1}} \\
&\rho = 10^{3}\ \mathrm{kg\,m^{-3}} && \mathcal{A} = 0.1\ \mathrm{nm\,ps^{-2}} \\
&C_v = 4 \times 10^{3}\ \mathrm{J\,kg^{-1}\,K^{-1}} && \Rightarrow \quad \mathcal{V} = 0.1\ \mathrm{nm\,ps^{-1}} \\
&l_z = 2\pi\ \mathrm{nm} && \tau_r = 1\ \mathrm{ps} \\
&\tau_c = 0.1\ \mathrm{ps} && T_s = 0.125\ \mathrm{K} \\
&s_{\max} = 1/10\ \mathrm{ps^{-1}}. &&
\end{aligned} \tag{27}$$

Thus for the requested shear rate we get a measurable value for $\mathcal{V}$ and a temperature shift of 0.125 K, which is negligible.

V. THE SLLOD ALGORITHM

One can also obtain the viscosity by imposing a Couette flow. The equation of motion needs to be modified to achieve this. In the SLLOD algorithm this is done in a non-Hamiltonian way. When shearing in the x-direction with the gradient in the z-direction, the SLLOD equations of motion are

$$\frac{d\mathbf{r}_i}{dt} = \mathbf{v}_i + s\, r_{i,z} \begin{pmatrix} 1 \\ 0 \\ 0 \end{pmatrix}, \tag{28}$$

$$\frac{d\mathbf{v}_i}{dt} = \frac{1}{m_i} \mathbf{f}_i - s\, v_{i,z} \begin{pmatrix} 1 \\ 0 \\ 0 \end{pmatrix}, \tag{29}$$

where i is the particle index, a second index indicates the vector component and s is the shear rate. As the system is periodic, the periodic boundary conditions also need to be modified. This can be accomplished by using a continuously deforming triclinic unit-cell, which is implemented in the GROMACS 3.0 package,[12] that we modified to use the SLLOD method. The viscosity is calculated from the stress tensor $\mathbf{P}$:

$$\eta = -\frac{1}{s} \langle P_{xz} \rangle. \tag{30}$$

There are two problems with this approach, besides the equations of motion not being Hamiltonian. The first problem is that conceptually the viscosity does not correspond to the viscosity obtained from an experiment. In the SLLOD algorithm not a force profile, but the linear velocity profile is imposed up to the atomic level, while in the experiment external forces induce a Couette flow on the macroscopic level. On the atomic level the velocity profile is not necessarily linear. In simple liquids these viscosities will be the same, but in complex liquids they can be different. A second problem is that the equations of motion produce an overall rotation in the system.

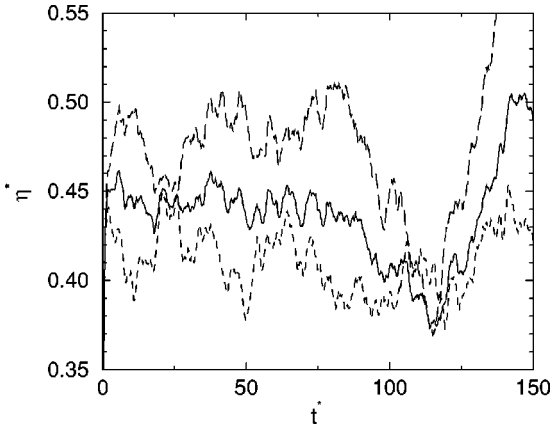

FIG. 1. Viscosity estimate for a Lennard-Jones fluid using Eq. (2). The derivative is plotted as a function of time for the whole simulation (solid line) and the two halves (dashed lines).

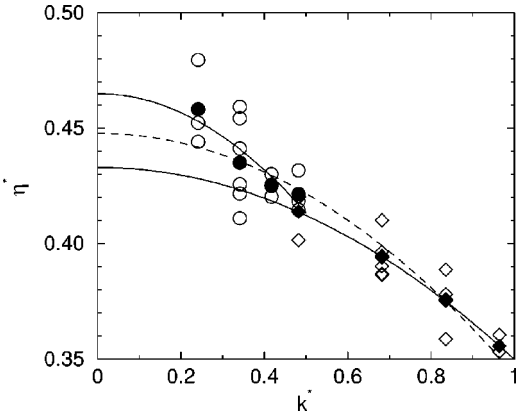

FIG. 2. Viscosity estimate for a Lennard-Jones fluid using transverse current autocorrelation functions. The circles are for the 8000 particle system; the diamonds for the 1000 particle system. The filled symbols are averages over all **k**-vectors (open symbols) with equal length. The solid lines are the fits to expression (13) for the separate systems; the dashed line is the fit for both systems.

VI. VISCOSITY OF A LENNARD-JONES FLUID

As a simple model system we chose a fluid of Lennard-Jones particles. The system was made dimensionless by expressing units in σ, ϵ and the mass. All simulations have been performed at number density $n^*=0.452$ and temperature $T^*=2$, starting from an equilibrated conformation. The time step was 0.01, the neighbor list was updated every 10 steps, with a cut-off of 5. The temperature was coupled using a Berendsen thermostat with a coupling time of 20.

For the pressure fluctuations method we performed a simulation in double precision with a duration of 5000 and in a periodic, cubic box containing 1000 particles. The right hand side of Eq. (2) averaged over the three off-diagonal elements, without taking the limit, is shown in Fig. 1. Since the curves are reasonably constant from $t^*=5$ to 80, we took the average over this period. An error estimate can be made from the three values for the off-diagonal elements. For the whole simulation the dimensionless viscosity η^* is 0.444 ± 0.018.

For the transverse-current method we simulated two systems for a duration of 5000: the system of 1000 particles described above and 8000 particles in a cubic box. The coordinates and velocities were written at intervals of 0.2. The **k**-vectors used for the analysis are (1,0,0), (1,1,0), (1, −1,0), (1,1,−1), (2,0,0) each in all 3 permutations and (1,1,1), for notational convenience we left out the inverse box length for each **k**-vector component. For each **k**-vector there are 2 perpendicular velocity directions and 2 amplitudes, one of $\sin(\mathbf{k}\cdot\mathbf{r})$ and one of $\cos(\mathbf{k}\cdot\mathbf{r})$. For each **k**-vector length there are only 3 independent directions. Since our simulation boxes are cubic, we can average over all permutations of the **k**-vectors given above, as well as over the **k**-vectors which differ only in signs. The transverse-current autocorrelation functions are close to exponential, except for the initial decay (not shown). A higher density would produce a negative minimum in the autocorrelation. The autocorrelation functions can be fitted very well with expression (10), where we used exponentially decaying weights with time constant 10. The resulting k-dependent viscosities of the 1000 particle system can be fitted perfectly with the second order approximation (13), this gives $\eta^*=0.433$ (Fig. 2). For the 8000 particle system the fit is worse; the value is $\eta^*=0.465$. Fitting one curve to both systems results in $\eta^*=0.448$. It is hard to tell which of these values is the best one. $\eta^*(k)$ will be closer to the real value of the viscosity for small k, but the error increases, since the correlation time is proportional to $1/k^2$.

For the periodic perturbation method we simulated systems of 3 different sizes, to study the wavelength dependence: 1000 particles in a cubic box as described above and 2 and 4 of these boxes stacked in the z-direction. The simulation protocol was the same as for the other methods, except for the coupling time of the Berendsen thermostat, which was set to 5, to more rapidly remove the energy introduced in the system by the external force. For each system size we used 3 different amplitudes for the acceleration profile. All simulations have length 5000. We started the analysis at time 400, which allows for enough time to develop a steady shear. Error estimates were calculated assuming a double exponential auto-correlation using formula (A16), which is derived in the Appendix. None of the simulations show a significant long correlation time. The short correlation time is close to τ_r [Eq. (7)]. All results are shown in Table I. The medium

TABLE I. Viscosity measurements of a Lennard-Jones fluid of N particles using the periodic perturbation method with 3 different system sizes. s^*_{max} and η^* are averages over time 400–5000. Two error estimates are given for the viscosity, one based on block averaging (see the Appendix) and between parentheses expression (25).

N	k^*	$\mathcal{A}^*$	s^*_{max}	η^*
1000	0.48	0.02	0.044	0.427 ± 0.019 (0.013)
		0.04	0.086	0.434 ± 0.007 (0.007)
		0.08	0.176	0.427 ± 0.005 (0.003)
2000	0.24	0.01	0.041	0.461 ± 0.014 (0.010)
		0.02	0.084	0.448 ± 0.004 (0.005)
		0.04	0.169	0.445 ± 0.005 (0.002)
4000	0.12	0.005	0.041	0.452 ± 0.006 (0.007)
		0.01	0.083	0.454 ± 0.004 (0.004)
		0.02	0.165	0.454 ± 0.002 (0.002)

and large systems give compatible values for the viscosity at all shear rates. The small system gives lower viscosities. This indicates the viscosity converges to the infinite wavelength value somewhere between $k^*=0.48$ and 0.24. The shear-rate dependence is negligible, since the highest shear rate (0.17) is still 15 times smaller than the inverse of the exponential decay time of the autocorrelation (1/0.4). The temperature shifts at $s_{\max}$ 0.08 and 0.17 are 0.5% and 2%, respectively. The most accurate estimate of the viscosity can be obtained from the large system, averaging the values for the 3 shear rates gives $\eta^*=0.453\pm0.002$.

For the SLLOD method we used the 1000 particle system with a shear rate of 0.05. The viscosity, averaged over time 400–5000 is 0.462 ± 0.008. The temperature shift is 0.4%.

To compare the accuracy at equal CPU-time, the runtime of the periodic perturbation simulations of 4000 particles should be decreased by a factor of 4. Taking into account the shear development time, the accuracy decreases by a factor 2.3, which makes the periodic perturbation method more accurate than both equilibrium methods at all 3 shear rates. At an equal average shear rate ($s_{\max}=2s$) the nonequilibrium methods are equally accurate.

VII. VISCOSITY OF THE SPC AND SPC/E WATER MODELS

To estimate the viscosity of the SPC (simple point charge) water model[13] from the pressure fluctuations, we have performed MD-simulations in double precision of 1728 molecules in a cubic box of length 3.75 nm. All simulations were done at a constant density of 980 kg m^{-3}. The temperature was coupled to 300 K, using a Berendsen thermostat[10] with a coupling time of 0.1 ps. The time step was 2 fs and the neighbor list, which is built with a cut-off of 0.9 nm, was updated every 5 steps. The cut-off for the Lennard-Jones interactions was 0.9 nm. The water geometry was maintained with the SETTLE algorithm.[14] We performed 5 simulations of 1 ns with different electrostatics treatments, starting from an equilibrated conformation. The first simulation used a Coulomb cut-off of 0.9 nm. The second simulation used a Coulomb cut-off of 1.4 nm, all forces between 0.9 and 1.4 nm were updated every 5 steps. The protocols for the third and fourth simulation are identical to the protocol of the first and second, respectively, except that a reaction field[15,16] with a dielectric constant of 80 was used. The fifth simulation used Particle Mesh Ewald (PME)[17] for the electrostatics, the cut-off for the particle–particle interactions was 0.9 nm. Because the simulations were performed at a constant volume, the pressure ranges from 3 bar for the 0.9 nm cut-off simulation to 500 bar for the 1.4 nm cut-off reaction-field simulation. The pressure fluctuations are about 270 bar for all 5 simulations. Running at a constant pressure of 1 bar would change the density by 1 or 2%, which would have little effect on the pressure fluctuations. To obtain the viscosity, we calculated the expression of Eq. (2), without taking the limit. The results for the 5 simulations are shown in Fig. 3. The differences between the simulations are large. This reflects the dependence of the pressure fluctuations on the treatment of the electrostatics. The long-range Coulomb interactions

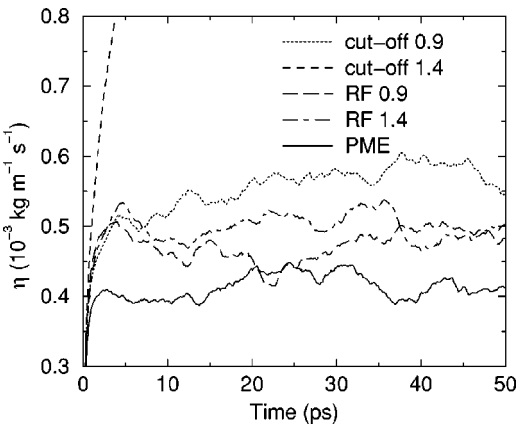

FIG. 3. Viscosity estimate for SPC water using Eq. (2). The derivative is plotted as a function of time for 5 simulations which differ only in electrostatics treatment.

have little effect on the potential, but the forces contribute significantly to the virial. Artifacts of the electrostatics cut-off can be seen in the dipole–dipole correlation plot (Fig. 4). At distances slightly below the cut-off the dipoles are anti-correlated, at distances slightly above the cut-off the dipoles are correlated. In addition to this effect, the simulation with a cut-off of 1.4 nm shows extra correlation at short distances. A reaction-field decreases the long-range correlations significantly. The reaction-field simulation with a cut-off of 0.9 nm has a lower dipole correlation in the first coordination sphere (0.28 nm). With PME there is no correlation after 0.75 nm. The too large correlation of dipoles at long distances makes an accurate estimation of the viscosity from pressure fluctuations impossible. A problem with all the simulations is that the derivative is not constant. Smith and Van Gunsteren applied the same method for a smaller system of 512 SPC water molecules using a cut-off of 0.9 nm.[18] They obtained viscosities of $0.54\pm0.09\cdot10^{-3}$ (kg m^{-1} s^{-1}) and $0.58\pm0.09\times10^{-3}$ with a reaction-field.

To check the convergence, we performed a simulation of 20 ns with PME, with a time step of 4 fs. The viscosity results are shown in Fig. 5. Still the pressure fluctuations look far from converged. We chose to average over time 1 to

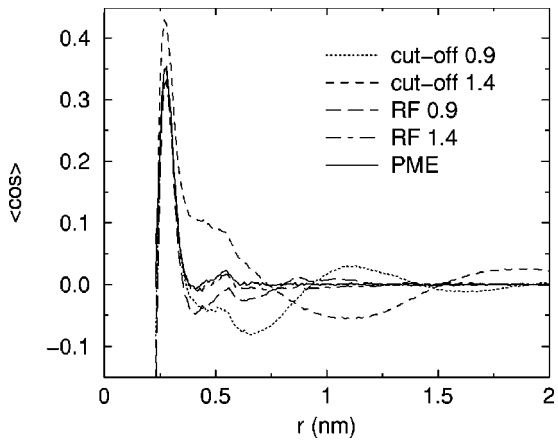

FIG. 4. The average inner product between the water dipole directions as a function of the distance between the dipoles.

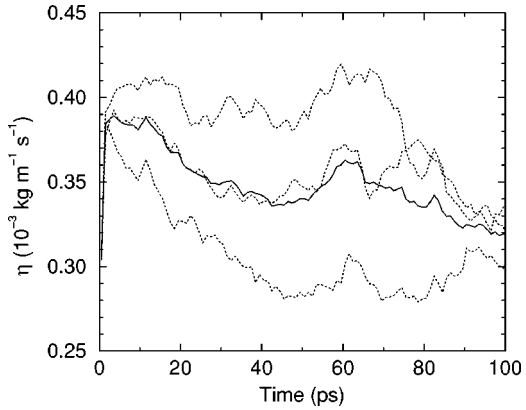

FIG. 5. Viscosity estimate for SPC water using Eq. (2). The derivative is plotted as a function of time for a simulation of 20 ns using PME. The dotted lines are the three off-diagonal elements of the pressure tensor; the solid line is the average.

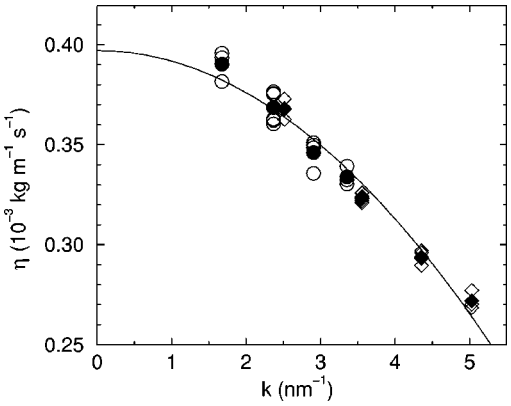

FIG. 7. Viscosity estimate for SPC water using transverse current autocorrelation functions. The circles are for the 1728 molecule system; the diamonds for the 512 molecule system. The filled symbols are averages over all **k**-vectors (open symbols) with equal length. The line is the fit of the filled symbols to expression (13).

20 ps, because the three off-diagonal elements are relatively close over this period. The resulting value for the viscosity is $0.38\pm0.02\times10^{-3}\,(\mathrm{kg\,m^{-1}\,s^{-1}})$. Note that even within these first 20 picoseconds the off-diagonal elements differ up to 10%.

To estimate the viscosity from the transverse-current correlation functions, we simulated the same system as above for 2 ns with PME. We used a coupling time of 2.5 ps instead of 0.1 ps for the Berendsen thermostat to minimize the influence of the thermostat on the correlation functions. The coordinates and velocities were written each 0.1 ps. To check the dependence of the viscosity on the size of the simulation box, we also simulated a system of 512 SPC water molecules at the same density with the same simulation protocol, coordinates and velocities were written every 0.05 ps. We calculated transverse current correlation functions using the center of mass of the water molecules. The transverse currents were calculated for the same **k**-vectors as for the Lennard-Jones fluid. Figure 6 shows the transverse-current autocorrelation functions as well as the fits for the 4 different **k**-vector lengths for the 1728 SPC system. Although the fit is better than a pure exponential fit, the first part of the curves is steeper than the fit and the negative part of the curves is also not fitted well. The values of the viscosity obtained from both simulations (Fig. 7) are consistent. Although a straight line fits the data much better, we fitted with the second order function (13), because the viscosity should be an even function of k. The resulting viscosity is $0.397\times10^{-3}\times(\mathrm{kg\,m^{-1}\,s^{-1}})$.

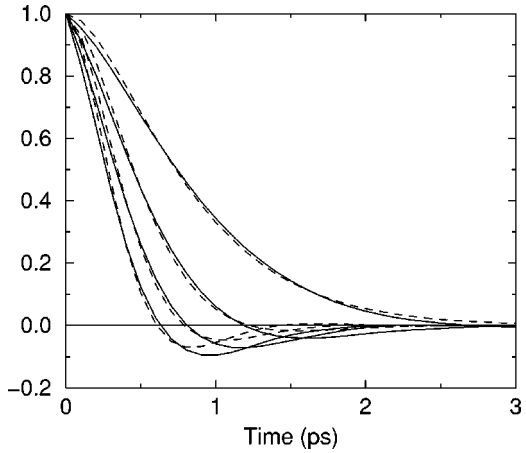

FIG. 6. Transverse current autocorrelation functions for the 1728 SPC molecule system for 4 different **k**-vector lengths. The solid lines are the correlation functions; the dashed lines the fit to expression (10).

We also measured the viscosity for several simulations of SPC water with the periodic perturbation method, using 3 different system sizes and several electrostatics treatments. The simulation protocol was identical to the one used for the equilibrium simulations described previously, except that each atom was subject to an additional acceleration according to Eq. (16). The system sizes, the electrostatics treatment and the results are shown in Table II. The accuracy of all simulations is in agreement with expression (25). The results for the smallest system show that the shear rate should not be higher than $0.1\,\mathrm{ps^{-1}}$; above this value the apparent viscosity starts to decrease and the temperature starts to increase. The simulations for the medium system size show the dependence of the viscosity on the electrostatics treatment and the temperature. The viscosity for the 2 cut-off simulations is 10% higher than PME simulation at 303 K and the reaction-field simulation with cut-off 0.9. The reaction-field simulation with twin-range cut-off is in between. The relative difference in the viscosity between the PME simulation at 300 and 303 K is two times as small as in experiment. For the large system the two cut-off simulations show that there is no dependence on the shear-rate at $0.026\,\mathrm{ps^{-1}}$. The PME simulation produces a viscosity of $0.405\pm0.005\times10^{-3}\,(\mathrm{kg\,m^{-1}\,s^{-1}})$. The same value is obtained when the viscosities of the PME simulations at the 3 different wavelengths are fitted to expression (13). The cut-off and PME simulations show the same k-dependence.

For the SLLOD method we simulated the 1728 SPC system mentioned above. The shear rate was $0.025\,\mathrm{ps^{-1}}$. The viscosity was obtained by averaging from 50 to 2000 ps. For a cut-off of 0.9 nm the viscosity is $0.423\pm0.010\times10^{-3}\,(\mathrm{kg\,m^{-1}\,s^{-1}})$, for PME electrostatics it is $0.407\pm0.007\cdot10^{-3}\,(\mathrm{kg\,m^{-1}\,s^{-1}})$.

TABLE II. Viscosity measurements using the periodic perturbation method with 3 different system sizes and experiment (Ref. 20). The first column shows the $x/y\times z$ dimensions of the simulation box, the number of molecules and the period used for analysis. c-o indicates cut-off treatment of the electrostatics, R_c is the cut-off distance. P (pressure), T_m (the measured temperature), s_{max} and η are averages over the period indicated in the first column. Two error estimates are given for the viscosity, one based on block averaging and between brackets expression (25). Note that T_m is a few degrees higher than the coupling temperature of 300 K for simulations without PME.

	Elec.	R_c (nm)	$\mathcal{A}$ (nm ps^{-2})	P (bar)	T_m (K)	s_{max} (ps^{-1})	η (10^{-3} kg m^{-1} s^{-1})
	c-o	0.9	0.025	42	302.4	0.053	0.414 ± 0.028 (0.026)
1.88×5.63 (nm)	c-o	0.9	0.05	62	302.5	0.107	0.412 ± 0.015 (0.013)
648 SPC	c-o	0.9	0.1	100	303.2	0.218	0.403 ± 0.010 (0.006)
20–200 (ps)	c-o	0.9	0.2	191	306.5	0.601	0.292 ± 0.004 (0.002)
	PME	0.9	0.05	322	300.2	0.113	0.388 ± 0.011 (0.012)
	c-o	0.9	0.025	43	302.5	0.067	0.436 ± 0.005 (0.004)
3.75×7.5 (nm)	c-o	1.4	0.025	−104	303.4	0.068	0.428 ± 0.005 (0.004)
3456 SPC	RF	0.9	0.025	498	303.3	0.076	0.388 ± 0.004 (0.003)
20–1000 (ps)	RF	1.4	0.025	388	302.9	0.072	0.406 ± 0.004 (0.004)
	PME	0.9	0.025	341	300.1	0.073	0.399 ± 0.003 (0.003)
	PME	0.9	0.025	389	303.1	0.076	0.387 ± 0.005 (0.003)
3.75×15 (nm)	c-o	0.9	0.0025	44	302.4	0.013	0.439 ± 0.010 (0.011)
6912 SPC	c-o	0.9	0.005	45	302.4	0.026	0.446 ± 0.006 (0.005)
50–2000 (ps)	PME	0.9	0.005	343	300.0	0.029	0.405 ± 0.005 (0.006)
3.75×15 (nm)		0.9	0.005	−166	300.0	0.018	0.642 ± 0.008 (0.009)
6912 SPC/E	PME						
50–2000 (ps)							
				1	300.2		0.851
experiment				1	302.2		0.815
				1	303.2		0.798

We performed one periodic perturbation simulation using a SPC/E (extended simple point charge) water model.[19] The simulation protocol is identical to the large SPC system with PME electrostatics. The only differences are that the oxygens have a charge of -0.8476 instead of -0.82 and the hydrogens have a charge of 0.4238 instead of 0.41. This small change in charge results in a viscosity of $0.642\pm0.008\times10^{-3}$ (kg m^{-1} s^{-1}), which is closer to the experimental value of 0.851×10^{-3} (kg m^{-1} s^{-1}).[20] Smith and van Gunsteren report values of $0.81\pm0.09\times10^{-3}$ (kg m^{-1} s^{-1}) and $0.91\pm0.07\times10^{-3}$ with the reaction-field, using the pressure fluctuation method.[18] The difference is caused by the error in the pressure fluctuations due to the cut-off treatment of the electrostatics, as was discussed above. The ratios of the values for the pressure fluctuation and the periodic perturbation method are the same as for SPC water.

VIII. CONCLUSIONS

We have compared four methods known from literature for calculating the shear viscosity from an MD-simulation. The methods differ in applicability, ease of use and computational cost. For a Lennard-Jones fluid, which has only short-range interactions, all four methods give reliable results. With a more complex liquid, such as water, both equilibrium methods have some problems.

The pressure fluctuations method requires accurate atomic forces, since these forces determine the virial and thus contribute to the pressure. To get accurate forces, the simulation should be performed in double precision. When Coulomb interactions are present, the long-range interactions should be treated accurately. Using a cut-off method, with a cut-off distance of 0.9 or 1.4 nm results in huge artifacts in the pressure fluctuations. This causes the calculated viscosity to be too high. A reaction-field reduces the artifacts, but only a long-range electrostatics method, such as PME, solves the problem completely. A second problem is choosing the period over which to average the integral of the pressure. This integral is very inaccurate for longer times. In general the averaging period can only be chosen after visual inspection.

The transverse current autocorrelation method is a more direct approach, since it is based on the decay of correlation in the motion of particles, which is directly related to the viscosity. This makes the method insensitive to the type of electrostatics treatment. A fit to an analytical transverse current autocorrelation function is required to obtain the viscosity. The Lennard-Jones fluid follows the behavior of the Navier–Stokes equation. A phenomenological correction using a simple memory function improves the fit slightly. The behavior of water is more complicated, even with the memory function the fit is not optimal. A more complex analytical model is needed to describe the behavior of all liquids. Thus far only the binary collision contribution to the transverse current correlation function has been derived.[21] Another problem is that the obtained viscosity depends on the wavelength, so extrapolation to infinite wavelength is required.

The periodic perturbation method is similar to the transverse-current autocorrelation method. The difference is that, instead of using internal fluctuations, a shear is induced. This allows for a larger signal to noise ratio, while the shear

rate can be chosen small enough that the structure and dynamics of the liquid are not disturbed. For a given simulation setup all relevant quantities can be estimated beforehand, including the simulation time required to reach a certain accuracy. The simulation box can be chosen to have an elongated shape such that the wavelength dependence of the viscosity becomes negligible. Thus only one simulation is required. Also a larger box produces better statistics. To obtain an accurate viscosity the shear rate should be an order of magnitude smaller than the inverse of the correlation time in the liquid. Under such conditions the method is still computationally more efficient then both equilibrium methods.

The SLLOD method has the same accuracy as the perturbation method at an equal average shear rate and equal computational time. However, it has several disadvantages. The equations of motion are non-Hamiltonian and the system has an overall rotation. But more importantly, the velocity is prescribed, which generates forces, instead of forces generating a velocity profile. In simple liquids this is not an issue, but for more complex ones it might become a problem. There is also the practical inconvenience of sliding boundary conditions.

Thus the periodic perturbation method is the method of choice, as it is insensitive to the electrostatics treatment and just as efficient as the SLLOD method, while it does not share the disadvantages of the SLLOD method.

APPENDIX: ERROR ESTIMATION

In this appendix we derive the standard error in the mean of a correlated fluctuating quantity. Consider an observable x, which fluctuates in time around an average value c:

$$x(t)=c+f(t), \tag{A1}$$

$$\langle f(t)\rangle=0. \tag{A2}$$

We want to estimate the error in the estimate of c, which we obtain by averaging $x(t)$ from $t=0$ to T. The optimal error estimate can be made when the autocorrelation of f is known:

$$\left\langle \left(\frac{1}{T}\int_0^T x(t)\mathrm{d}t - c \right)^2 \right\rangle = \frac{1}{T^2}\left\langle \left(\int_0^T f(t)\mathrm{d}t \right)^2 \right\rangle = \frac{1}{T^2}\int_0^T\int_0^T \langle f(t)f(u)\rangle \mathrm{d}u\,\mathrm{d}t. \tag{A3}$$

When it is unknown, the autocorrelation can be fitted to a given functional form. However, usually autocorrelation functions have long tails, which complicates the fitting. It is better to fit an integral property of f. One integral property is the error estimate from a block average. The data can be divided into N blocks, over which the average is calculated. When the block averages are considered to be independent, a standard error estimate S can be calculated by dividing the standard deviation of these averages by $\sqrt{N}$:

$$S^2(N)=\frac{1}{N}\frac{1}{(N-1)}\times\sum_{i=1}^{N}\left(\frac{N}{T}\int_{[(i-1)/N]\,T}^{(i/N)\,T} x(t)\mathrm{d}t - \frac{1}{T}\int_0^T x(t)\mathrm{d}t \right)^2. \tag{A4}$$

When the block length is shorter than the correlation time of f, the error estimate will be too low. When T is much longer than the correlation time, the error estimate will be almost exact. The expectation of $S^2(N)$ can be calculated analytically:

$$\langle S^2(N)\rangle=\frac{1}{N}\frac{1}{(N-1)}\times\left\langle \sum_{i=1}^{N}\left(\frac{N}{T}\int_{[(i-1)/N]\,T}^{(i/N)\,T} x(t)\mathrm{d}t - \frac{1}{T}\int_0^T x(t)\mathrm{d}t \right)^2 \right\rangle \tag{A5}$$

$$=\frac{1}{N(N-1)}\left\langle \sum_{i=1}^{N}\left(\left(\frac{N}{T}\int_{[(i-1)/N]\,T}^{(i/N)\,T} f(t)\mathrm{d}t \right)^2 - \left(\frac{1}{T}\int_0^T f(t)\mathrm{d}t \right)^2 \right) \right\rangle \tag{A6}$$

$$=\frac{1}{N-1}\left(\left\langle \left(\frac{N}{T}\int_0^{T/N} f(t)\mathrm{d}t \right)^2 \right\rangle - \left\langle \left(\frac{1}{T}\int_0^T f(t)\mathrm{d}t \right)^2 \right\rangle \right) \tag{A7}$$

$$=\frac{1}{N-1}\left(\frac{N^2}{T^2}\int_0^{T/N}\int_0^{T/N}\langle f(t)f(u)\rangle \mathrm{d}u\,\mathrm{d}t - \frac{1}{T^2}\int_0^T\int_0^T \langle f(t)f(u)\rangle \mathrm{d}u\,\mathrm{d}t \right). \tag{A8}$$

So the expectation can be calculated when the autocorrelation of f is known. When the autocorrelation is exponential,

$$\langle f(t)f(u)\rangle=\sigma^2\exp\left(-\frac{|t-u|}{\tau} \right), \tag{A9}$$

the expectation of $S^2(N)$ appears to be

$$\langle S^2(N)\rangle=\frac{2\sigma^2\tau}{T}\left(1+\frac{N\tau}{T}\left(\exp\left(-\frac{T}{N\tau} \right)-1 \right) \right. \tag{A10}$$

$$\left. +\frac{\tau}{T}\frac{N}{N-1}\left(\exp\left(-\frac{T}{N\tau} \right)-1+\frac{1}{N} \right.\right. \times\left.\left. \exp\left(-\frac{T}{\tau} \right)-\frac{1}{N} \right) \right), \tag{A11}$$

$$=\frac{2\sigma^2\tau}{T}\left(1+\frac{N\tau}{T}\left(\exp\left(-\frac{T}{N\tau} \right)-1 \right)+O\left(\frac{\tau}{T} \right) \right). \tag{A12}$$

When T is larger than the correlation time τ, the last term can be neglected. When T is of the order of τ the observation time is not sufficient to estimate the error. We can also write the error estimate in terms of the block length $t=T/N$:

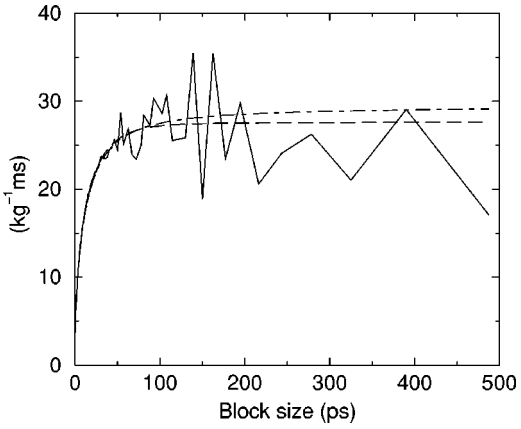

FIG. 8. Error estimates for $1/\eta$ for the 6912 SPC system with cut-off electrostatics and $\mathcal{A}=0.005$ nm/ps^{-2}. The analysis was done from 50 to 2000 ps (19501 data points). The standard deviation of $1/\eta$ is 253. All curves are plotted as a function of the block length, which is $1950/N$ ps, where N is the number of blocks. The solid curve is the error estimate $S(N)$ assuming the blocks are independent [expression (A4)]. The dashed curve is the fit using $\mathcal{E}(t)$ [expression (A16)]. The coefficient of the slow exponential is negative; this is due to bad statistics when using a small number of blocks. To obtain a more accurate error estimate, we fitted again with a single exponential, this is the dot–dashed curve ($\tau=13.3$ ps). This gives a standard error estimate for $1/\eta$ of 29.5.

$$\langle S^2(t)\rangle = \frac{2\sigma^2\tau}{T}\left(1+\frac{\tau}{t}\left(\exp\left(-\frac{t}{\tau}\right)-1\right)+O\left(\frac{\tau}{T}\right)\right). \tag{A13}$$

A single exponential autocorrelation can usually be fitted easily, but problems arise when there is a second, longer correlation time present in f:

$$\langle f(t)f(u)\rangle = \sigma^2\left(\alpha\exp\left(-\frac{|t-u|}{\tau_1}\right)+(1-\alpha)\times\exp\left(-\frac{|t-u|}{\tau_2}\right)\right). \tag{A14}$$

Usually one decay time, which we choose to be τ_2, is at least one order of magnitude larger than the other and α is very close to 1. The expectation now becomes

$$\langle S^2(t)\rangle = \frac{2\sigma^2}{T}\left(\alpha\tau_1\left(1+\frac{\tau_1}{t}\left(\exp\left(-\frac{t}{\tau_1}\right)-1\right)\right)+(1-\alpha)\tau_2\left(1+\frac{\tau_2}{t}\left(\exp\left(-\frac{t}{\tau_2}\right)-1\right)\right)+O\left(\frac{\tau_1^2}{T}\right)+O\left(\frac{\tau_2^2}{T}\right)\right). \tag{A15}$$

When we neglect the last 2 terms, we obtain a relatively simple function $\mathcal{E}$ which depends on T as $1/\sqrt{T}$:

$$\mathcal{E}^2(t) = \frac{2\sigma^2}{T}\left(\alpha\tau_1\left(1+\frac{\tau_1}{t}\left(\exp\left(-\frac{t}{\tau_1}\right)-1\right)\right)+(1-\alpha)\tau_2\left(1+\frac{\tau_2}{t}\left(\exp\left(-\frac{t}{\tau_2}\right)-1\right)\right)\right). \tag{A16}$$

The optimal error estimate [Eq. (A3)] is given by the limiting value of $\mathcal{E}(t)$:

$$\lim_{t\to\infty}\ \mathcal{E}(t)=\sigma\sqrt{\frac{2(\alpha\tau_1+(1-\alpha)\tau_2)}{T}}. \tag{A17}$$

To estimate the error one needs to estimate σ, α, τ_1 and τ_2. The standard deviation of $x(t)$ over time $t=0$ to T provides the optimal estimate for σ. The other 3 parameters can be obtained from a fit of $S(t)$ to $\mathcal{E}(t)$. There are restrictions on the range of the fitting parameters: α should be between 0 and 1 and τ_1 and τ_2 should be larger than 0. When the longest correlation time, τ_2, is longer than the averaging interval and $(1-\alpha)\tau_2$ is not negligible compared to $\alpha\tau_1$, there is not enough statistics to estimate the error. An example is given in Fig. 8.

[1] B. J. Palmer, Phys. Rev. E **49**, 359 (1994).
[2] G. Ciccotti, G. Jacucci, and I. R. McDonald, J. Stat. Phys. **21**, 1 (1979).
[3] The name SLLOD originates from the use of the transposed Doll's tensor, the dyadic product **q p** of positions and momenta, which was named after the Kewpie Doll by Hoover.
[4] D. J. Evans and G. P. Morriss, *Statistical Mechanics of Nonequilibrium Liquids* (Academic, London, 1990).
[5] M. P. Allen and D. J. Tildesley, *Computer Simulations of Liquids* (Oxford Science Publications, Oxford, 1987).
[6] G. Arya, E. J. Maginn, and H.-C. Chang, J. Chem. Phys. **113**, 2079 (2000).
[7] R. Zwanzig, Annu. Rev. Phys. Chem. **16**, 67 (1965).
[8] D. Forster, *Hydrodynamics, Fluctuations, Broken Symmetry and Correlation Functions* (Benjamin/Cummings, Reading, MA, 1975).
[9] J. P. Boon and S. Yip, *Molecular Hydrodynamics* (Dover, New York, 1991).
[10] H. J. C. Berendsen, J. P. M. Postma, W. F. van Gunsteren, A. DiNola, and J. R. Haak, J. Chem. Phys. **81**, 3684 (1984).
[11] H. J. C. Berendsen, "Transport properties computed by linear response through weak coupling to a bath," in *Computer Simulations in Material Science*, edited by M. Meyer and V. Pontikis (Kluwer, Dordrecht, 1991), pp. 139–155.
[12] E. Lindahl, B. Hess, and D. van der Spoel, J. Mol. Model. [Electronic Publication] **7**, 306 (2001).
[13] H. J. C. Berendsen, J. P. M. Postma, W. F. van Gunsteren, and J. Hermans, "Interaction models for water in relation to protein hydration," in *Intermolecular Forces*, edited by B. Pullman (Reidel, Dordrecht, 1981), pp. 331–342.
[14] S. Miyamoto and P. A. Kollman, J. Comput. Chem. **13**, 952 (1992).
[15] R. O. Watts, Mol. Phys. **28**, 1069 (1974).
[16] M. Neumann and O. Steinhauser, Mol. Phys. **39**, 437 (1980).
[17] T. Darden, D. York, and L. Pedersen, J. Chem. Phys. **98**, 10089 (1993).
[18] P. E. Smith and W. F. van Gunsteren, Chem. Phys. Lett. **215**, 315 (1993).
[19] H. J. C. Berendsen, J. R. Grigera, and T. P. Straatsma, J. Phys. Chem. **91**, 6269 (1987).
[20] R. C. Weast, in *CRC Handbook of Chemistry and Physics* (CRC Press, Boca Raton, 1986).
[21] R. K. Sharma, K. Tankeshwar, K. N. Pathak, S. Ranganathan, and R. E. Johnson, J. Chem. Phys. **108**, 2919 (1998).